

## Energy Exchange between Mesoparticles and Their Internal Degrees of Freedom

Alejandro Strachan and Brad Lee Holian

*Theoretical Division, Los Alamos National Laboratory, Los Alamos, New Mexico 87545, USA*

(Received 18 March 2004; published 7 January 2005)

We present mesoscale equations of motion that lead to a thermodynamically accurate description of the energy exchange between mesoparticles and their internal degrees of freedom. In our approach, energy exchange is done through particle coordinates, rather than momenta, resulting in Galilean invariant equations of motion. The total linear momentum and total energy (including the internal energy of the mesoparticles) are conserved, and no coupling occurs when a mesoparticle is in free flight. We test our method for shock wave propagation in a crystalline polymer, poly(vinylidene fluoride); the mesodynamics results agree very well with all-atom molecular dynamics.

DOI: 10.1103/PhysRevLett.94.014301

PACS numbers: 45.10.-b, 62.20.-x, 62.50.+p

Large-scale atomistic simulations enable a detailed understanding of complex, many-body problems in physics, chemistry, materials science, and biology. Unfortunately, despite the advances in methodologies and computer power, a wide range of phenomena is beyond present capabilities. In many of these cases, all-atom molecular-dynamics (MD) simulations are neither necessary nor desirable: coarse-grained descriptions of matter, where groups of atoms are described by a single mesoparticle, ought to provide the required detail in a computationally efficient manner. The first task of mesodynamics is to describe the nonlinear elastic behavior under compression, as well as the tensile failure, by a realistic mesopotential between the mesoparticles [1]. These mesoparticles can represent atoms and their electronic degrees of freedom (DOFs) in metallic systems [2], molecular groups in polymers [3], molecules in molecular crystals, or grains in polycrystalline metals [1]. While these approaches can be formulated to give accurate treatment of mechanical properties, there has been, up to now, no realistic thermomechanical treatment of the energy exchange between the mesoparticle and its DOFs: their thermal role has been either completely disregarded or treated only crudely.

The propagation of shock waves in molecular crystals is particularly challenging to a mesodynamics description, since high energies and fast processes are involved. (Full atomistic shock simulations are also computationally very expensive.) The shock wave initially excites long-wavelength, low-energy intermolecular DOFs (the ones described explicitly at the mesoscale), resulting in short-lived overheating of these (few) modes. Part of this energy then “cascades” to higher-energy, higher-frequency intramolecular DOFs, which are only implicitly treated in mesoscopic descriptions, on a time scale that depends on the details of the molecular vibrational spectrum. This equilibration process continues until the internal and molecular temperatures reach the same value. One hopes to formulate mesodynamics that accurately predicts the final shocked-state temperature, internal energy, and pressure.

In this Letter, we present equations of motion for mesodynamics that lead to a thermodynamically accurate description of energy exchange between mesoparticles and their internal DOFs. Dissipation in particle-based macroscale simulations, such as smooth particle hydrodynamics (SPH) [4], has been discussed by Hoover [in his more general version of SPH, known as smooth particle applied mechanics [5]]. In these macroscale particle methods and in our earlier mesodynamics formulation, the local velocity  $\langle \mathbf{u} \rangle_i$  in the neighborhood of a given particle  $i$  is defined in terms of its own velocity and the velocities of its neighbors  $\mathbf{u}_j$ , averaging over the neighborhood with a short-range weighting function  $w(r_{ij})$  that decays monotonically with interparticle distance  $r_{ij} = |\mathbf{r}_i - \mathbf{r}_j|$ :

$$\langle \mathbf{u} \rangle_i = \frac{\sum_j w(r_{ij}) m_j \mathbf{u}_j}{\sum_j w(r_{ij}) m_j}, \quad (1)$$

where the sum is over all particles. By analogy, the local neighborhood temperature  $T_i$  in  $d$  spatial dimensions is given by

$$dT_i = \frac{\sum_j w(r_{ij}) m_j |\mathbf{u}_j - \langle \mathbf{u} \rangle_i|^2}{\sum_j w(r_{ij})}. \quad (2)$$

(See the supplementary material [6] for the weighting function used in this Letter.)

In Monaghan’s SPH equations [7] particle positions are updated using the neighborhood velocity  $\langle \mathbf{u} \rangle_i$  rather than their own particle velocities  $\mathbf{u}_i$ . In our earlier version of mesodynamics [1], we proposed the use of relative-velocity viscous damping [8] as a place holder for a more sophisticated treatment of energy exchange. While both of these dissipative approaches allow particles that have broken free from their neighbors to fly ballistically without slowing down, the mesoparticle temperature  $T_i$  always tends toward zero regardless of the process being simulated. However, in the thermomechanical meso-

dynamics equations of motion, the local energy of the mesoparticle must be *exchanged* with that in the internal DOFs in a Galilean invariant manner, by which we mean that the addition of a constant velocity to all mesoparticles must have no effect upon the update of either the mesoparticle velocity or its internal temperature. A consequence of Galilean invariance is that the common practice of adding a viscous-damping deceleration term to the velocity update equation cannot be justified.

In the mesodynamics equations of motion, we couple the local mesoparticle temperature  $T_i$  in the vicinity of particle  $i$  to its internal temperature  $T_i^0$  by means of an additional dissipative contribution to the mesoparticle velocity in the coordinate update equation (rather than adding a viscous deceleration in the velocity update, as is customary in all other thermostatting techniques). The dissipative term contains a factor proportional to the temperature difference between internal and mesoscopic DOFs. The thermal energy of the internal DOFs is described via their specific heat  $C_i^0$ , which is in general a function of  $T_i^0$ . The mesodynamics equations of motion are then given by

$$\begin{aligned}\dot{\mathbf{r}}_i &= \mathbf{u}_i + \nu \left( \frac{T_i - T_i^0}{\theta^0} \right) \frac{\mathbf{F}_i}{m_i \langle \omega^2 \rangle}, \\ \dot{\mathbf{u}}_i &= \frac{\mathbf{F}_i}{m_i}, \\ \dot{T}_i^0 &= \nu \left( \frac{T_i - T_i^0}{\theta^0} \right) \frac{|\mathbf{F}_i|^2}{C_i^0 m_i \langle \omega^2 \rangle},\end{aligned}\quad (3)$$

where  $\nu$  is a coupling rate that determines the time scale of equilibration between internal and external DOFs (it can be obtained by requiring the mesoscale description to match the equilibration rate of all-atom simulations). The temperature difference  $T_i - T_i^0$  controls the sign of the energy exchange, similar to the Berendsen thermostat [9];  $\theta^0$  is a reference temperature (in our simulations,  $\theta^0 = 300$  K). Note that we do *not* write the temperature difference as it usually appears in the Berendsen thermostat equations of motion (namely,  $1 - T_i^0/T_i$ ) for two reasons: (1) since the thermostat is “finite,” i.e., both temperatures change when energy is exchanged, the Berendsen form, with its ratio of  $T_i^0$  to  $T_i$ , cannot guarantee that both temperatures will converge to the same value; (2) since  $T_i \rightarrow 0$  in the ballistic limit, the Berendsen expression is ill defined. The total force  $\mathbf{F}_i$  on particle  $i$  is obtained from the mesopotential, and  $\langle \omega^2 \rangle$  is the mean-square (Einstein) frequency of the mesoparticle vibrational modes. If  $T_i > T_i^0$  the coupling will appropriately transfer energy from the external to the internal DOFs; if  $T_i < T_i^0$ ,  $T_i^0$  will decrease, according to the last of Eqs. (3). This equation for  $\dot{T}_i^0$  ensures that the total energy (mesoparticle plus internal) is conserved. (See the supplementary material [6] for an algorithm for numerical integration of the mesodynamics equations of motion.)

In summary, the mesodynamics equations of motion [Eqs. (3)] satisfy the following properties: (i) the total energy and momentum of the system (mesoparticles plus internal DOFs) are conserved; (ii) energy exchange is done on a spatially local basis; (iii) the ballistic regime is handled correctly—an isolated particle moves at a constant velocity with no force on it and exchanges no energy with its internal DOFs; (iv) the equations of motion are Galilean invariant; (v) and, as the coupling between internal and external modes is reduced to zero, Newton’s (Hamilton’s) equations of motion are recovered. We point out that the Berendsen-like (i.e., *time irreversible*) thermostatting technique we have introduced here can be generalized to integral feedback that is completely *time reversible* [10]. Moreover, we show that this integral feedback, when specialized to an infinite number of internal DOFs, is consistent with the canonical ensemble, in a manner reminiscent of the Nosé-Hoover thermostat [11].

As an example of this new mesodynamics with internal thermostats, we report here on shock wave propagation in the crystalline polymer poly (vinylidene fluoride) (PVDF), with monomer  $\text{CH}_2\text{-CF}_2$  in its  $\beta$  phase (a polar crystal with all-trans bonds). The crystal is formed by infinite, parallel chains. In the plane perpendicular to the chains, it forms a quasihexagonal phase [12]; see Fig. 1. We choose the axes of our simulation cells such that the chains are oriented along the  $z$  direction and the dipole moment of each chain is along the  $y$  direction; we study shock propagation in the  $x$  direction.

The all-atom MD simulations reported in this Letter were performed using a vibrationally accurate force field, denoted MSXX [13]. For the mesodynamics simulations, we represent each polymer chain by one mesoparticle in two dimensions (retaining  $x$  and  $y$  directions). The interaction between mesoparticles is a pairwise-additive Rydberg potential that reproduces the stress in uniaxial compression (along the  $x$  direction) of the all-atom MSXX version of PVDF; the inset of Fig. 2 shows the  $xx$  component of the zero-temperature 2D stress (stress times the unit-cell length in the  $z$  direction) as a function of

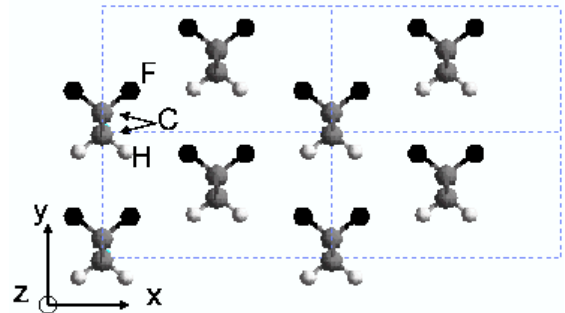


FIG. 1 (color online). PVDF crystal structure. We show the  $xy$  projection of four unit cells. Each cell contains two infinite chains (periodic in the  $z$  direction). The crystal is three dimensional: the  $\text{CH}_2$  and  $\text{CF}_2$  groups are in different  $xy$  planes.

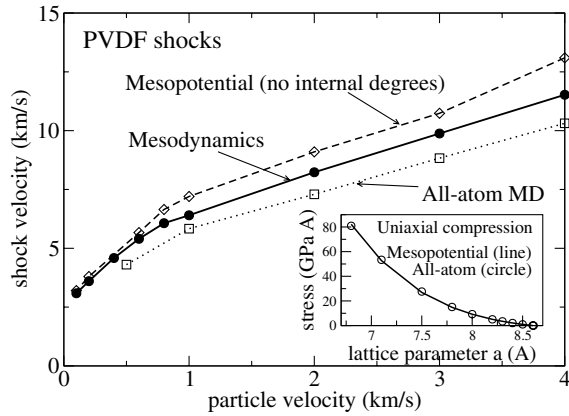


FIG. 2. Shock velocity as a function of particle velocity for PVDF: all-atom simulation (squares); bare mesopotential without coupling to implicit DOFs (diamonds); and mesodynamics with a coupling constant  $\nu = 0.1$  (solid circles). Inset shows stress-strain curves for uniaxial compression of PVDF obtained using the MSXX force field in all-atom simulations (circles) and the mesopotential (line).

uniaxial compression, both from all-atom MD simulations and from our mesopotential (see supplementary material [6] for details). We assume, for simplicity, that the internal specific heat of the mesoparticles is given by the classical harmonic approximation  $C_i^0/k = N_{\text{int}}$ , where  $N_{\text{int}}$  is the number of internal DOFs. At the mesoscale, each chain is described by a single (2D) mesoparticle that contains  $N = 6$  atoms (in 3D), so that  $N_{\text{int}} = 6 \times 3 - 2 = 16$ . We calculated the mean-square frequency from the vibrational density of states, using spectral analysis of MD velocities at normal density and temperature (300 K):  $\langle \omega^2 \rangle = 222 \text{ ps}^{-2}$ . The coupling constant  $\nu = 0.1$  leads to a reasonable description of equilibration during shock loading, as is shown below.

We study shock propagation using high-velocity impact nonequilibrium MD simulations, with piston velocities between 0.1 and 4 km/s for mesodynamics and between 0.5 and 4 km/s for the all-atom description. Figure 2 shows the resulting shock velocity ( $u_s$ ) as a function of particle velocity ( $u_p$ ) obtained from all-atom MD and mesodynamics. In order to characterize the effect of the implicit DOFs on  $u_s$ , we also show in Fig. 2 the results using the mesopotential, but with no coupling to internal DOFs, i.e., simply solving Newton's equations of motion, with forces given by the mesopotential. We see that the mesopotential accurately reproduces the Hugoniot  $u_s$ - $u_p$  states for weak shocks and qualitatively describes its general features. It was designed to describe elastic properties (including anharmonicities), but was not intended to capture complex phenomena like plasticity and structural transitions at high  $u_p$ .

Figure 3 shows the shock rise of the local temperature of a thin slab of material (one unit cell wide) as a shock wave with  $u_p = 3 \text{ km/s}$  passes through it. In the all-atom MD

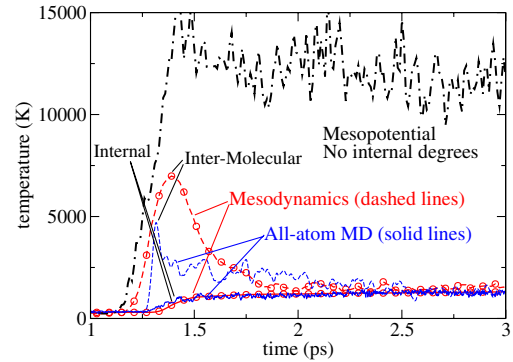


FIG. 3 (color online). Time dependence of the local temperature of a thin slab of PVDF as a shock passes through (particle velocity  $u_p = 3 \text{ km/s}$ ). We show inter- and intramolecular temperatures for all-atom MD, as well as mesodynamics, both with and without coupling to internal modes.

simulations, we obtain two types of local temperatures: (1) the *intermolecular* temperature, defined as the fluctuations of the c.m. velocities of each polymer chain around the c.m. translational velocity of the whole slab, and (2) the *internal* temperature, defined as atomic velocity fluctuations around the c.m. velocity of each molecule. The two all-atom temperatures have well defined counterparts in the mesoscopic description; the internal temperature is just  $T_i^0$ , and the intermolecular temperature  $T_i$  is calculated from the velocity of the mesoparticles. The all-atom MD simulation shows that the shock wave initially excites the long-wavelength molecular modes; thus, the intermolecular temperature (dashed line) rises faster than the internal temperature (solid line) and initially overshoots its final value. As the higher-frequency internal DOFs get excited, intermolecular and intramolecular DOFs equilibrate, and both temperatures converge to the same value. We also show in Fig. 3 the temperature evolution obtained with our mesopotential, both with coupling to the internal DOFs (circles) and without (dash-dotted line). As one would expect, the bare mesopotential without coupling greatly overestimates the final temperature, due to the reduced number of DOFs available to accommodate the energy increase. This clearly shows how important energy exchange is to a correct formulation of mesodynamics: the new mesoscopic dynamics correctly predicts the final temperature and rise times of the shocked material.

Figure 4 shows the time evolution of the internal temperature for various shock strengths (from  $u_p = 1$  to 4 km/s) obtained from both all-atom MD simulations and mesodynamics. The mesoscopic description leads to very accurate final temperatures and a good description of rise times for all cases. Remember that the only free parameter in our new thermomechanical version of mesodynamics is the coupling strength between internal and external (mesoscale) DOFs ( $\nu$ )—we use the same value for all cases. Mesodynamics slightly overestimates final temperatures, since the mesopotential overestimates the

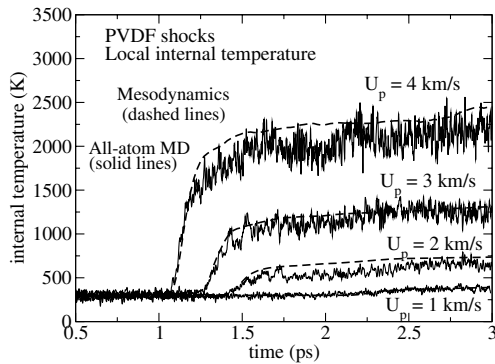


FIG. 4. Time dependence of the internal temperature of a thin PVDF slab for shocks of various strengths: all-atom simulations (solid lines) and mesodynamics (dashed lines).

shock velocity for high-strength shocks. (From the Rankine-Hugoniot jump conditions, one can see that a higher shock velocity leads to higher total energy in the shocked material and consequently a higher temperature.)

We have presented in this Letter the simplest implementation of a thermodynamically accurate set of mesodynamics equations of motion. The main approximation is that internal modes exchange energy with the mesoparticles by a single, average, relaxation rate; this leads to slight discrepancies in the overshoot of the intermolecular temperature at early times. One can easily make this a two-rate internal process, where high-energy modes take longer to get excited (small  $\nu_1$ ) and floppy modes are excited more rapidly (larger  $\nu_2$ ), along with the corresponding internal temperatures,  $T_i^{0(1)}$  and  $T_i^{0(2)}$ . It is also important to point out that the specific heat used to describe the thermodynamics of the internal DOFs can be accurately obtained from the vibrational spectra of the corresponding molecule or fragment. Furthermore, the specific heat can be based on quantum (rather than classical) statistical mechanics. In this way, the high-energy modes will not be populated for low temperatures—weak shocks in our example—leading to a smaller number of “effective” DOFs and consequently higher final temperatures. All-atom MD is completely classical in nature, so that mesodynamics with an accurate specific heat can, surprisingly, lead to more accurate results than all-atom MD. We also note that, in MD simulations of metallic systems, our treatment of the implicit DOFs (with a straightforward modification that allows heat exchange between the internal DOFs of neigh-

boring mesoparticles) can be used to describe the thermal and transport role of electronic DOFs [10].

The new thermomechanical formulation of mesodynamics presented in this Letter is generally applicable, extending the spatial and temporal ranges of more expensive all-atom simulations to thermodynamically realistic mesoscopic simulations, with the possibility of solving a wide variety of problems in physics, chemistry, materials science, and biology.

This work was supported by the ASC Materials and Physics Modeling Program at Los Alamos.

- 
- [1] B. L. Holian, *Europhys. Lett.* **64**, 330 (2003).
  - [2] H. Häkkinen and U. Landman, *Phys. Rev. Lett.* **71**, 1023 (1993).
  - [3] Florian Muller-Plathe, *Chem. Phys. Chem.* **3**, 754 (2002); K. Fremer, *Macromol. Chem. Phys.* **204**, 257 (2003).
  - [4] L. Lucy, *Astron. J.* **82**, 1013 (1977); J. J. Monaghan, *Annu. Rev. Astron. Astrophys.* **30**, 543 (1992).
  - [5] O. Kum, W. G. Hoover, and H. A. Posch, *Phys. Rev. E* **52**, 4899 (1995).
  - [6] See EPAPS Document No. E-PRLTAO-94-054503 for the following: (i) A description of the mesopotential used to describe the interactions between poly(vinylidene fluoride) (PVDF) molecules. (ii) The weighting function used to calculate local temperature and velocity of the mesoparticles. (iii) An algorithm to integrate the new mesodynamics equations of motion. A direct link to this document may be found in the online article’s HTML reference section. The document may also be reached via the EPAPS homepage (<http://www.aip.org/pubservs/epaps.html>) or from <ftp.aip.org> in the directory /epaps/. See the EPAPS homepage for more information.
  - [7] J. J. Monaghan, *J. Comput. Phys.* **82**, 1 (1989); J. P. Gray, J. J. Monaghan, and R. P. Swift, *Comput. Methods Appl. Mech. Eng.* **190**, 6641 (2001).
  - [8] O. B. Firsov, *Sov. Phys. JETP* **9**, 1076 (1959); M. Moseler, J. Nordiek, and H. Haberland, *Phys. Rev. B* **56**, 15 439 (1997).
  - [9] H. Berendsen, J. Postma, W. van Gunsteren, A. Dinola, and J. Haak, *J. Chem. Phys.* **81**, 3684 (1984).
  - [10] A. Strachan, T. C. Germann, and B. L. Holian (to be published).
  - [11] B. L. Holian, A. F. Voter, and R. Ravelo, *Phys. Rev. E* **52**, 2338 (1995).
  - [12] T. Furukawa, *Phase Transit.* **18**, 143 (1989).
  - [13] N. Karasawa and W. A. Goddard III, *Macromolecules* **25**, 7268 (1992).